Reactions of Laser-Ablated Scandium Atoms with Nitrogen: Matrix Infrared Spectra and DFT Calculations for Scandium Nitrides and the Fixation of Nitrogen by Two Scandium Atoms

George V. Chertihin,[†] Lester Andrews,*[,†] and Charles W. Bauschlicher, Jr.[‡]

Contribution from the Department of Chemistry University of Virginia, Charlottesville, Virginia 22901, and STC-230-3, NASA Ames Research Center, Moffett Field, California 94035

Received October 24, 1997

Abstract: Laser-ablated Sc atoms react with nitrogen to form ScN, $Sc(N_2)$ and $(ScN)_2$ and their N_2-ligated counterparts. These identifications are based on nitrogen-15 isotopic shifts and agreement with DFT vibrational frequency calculations. It is noteworthy that annealed argon matrix samples containing 2% N_2 give almost the same absorptions as nitrogen matrix samples for the ligated complexes $(NN)_xScN$ and $(ScN)_2(NN)_x$. The rhombic $(ScN)_2$ molecule is made by reaction of a second Sc atom with an intermediate ScN_2 species and, thus, provides a method of nitrogen fixation with naked metal atoms.

Introduction

Little is known experimentally about first-row transition metal nitride molecules with the exception of TiN,[1,2] VN,[3,4] and CrN,[5] and only mass and emission spectra with rotational analysis[6,7] have been reported for molecular ScN. The solid material is hard, refractory, and electrically conducting.[8,9] The most recent ab initio calculations predict a formal triple bond[10] and a harmonic frequency near 770 cm^{-1} for ScN although earlier calculations revealed only weak bonding.[11] Scandium holds a special place in the role of transition metal chemistry because Sc contains the smallest number of electrons, there are three low-lying electron configurations ($3d^14s^2$, $3d^24s^1$, $3d^14s^14p^1$), and the 4s and 3d orbitals have similar radial extent and may simultaneously participate in bonding. This latter point is demonstrated by the recent observation of scandium dioxide, OScO, with an antisymmetric stretching fundamental between that for OTiO, where double bonds are present, and for OCaO, where only single bonds can form.[12]

Laser-ablated transition metal atoms contain sufficient excess energy to dissociate molecular nitrogen, and direct metal and nitrogen atom combination during sample condensation leads to the formation of MN molecules in both argon and nitrogen matrixes. In the first application of this technology, FeN was observed at 938.0 cm^{-1} in solid argon and at 934.8 cm^{-1} in solid nitrogen based on nitrogen isotopic shifts.[13] Subsequent work with Ti, V, Cr, Mn, and Co, Ni has identified both the isolated MN molecules as well as a series of $(NN)_xMN$ complexes in solid argon and the saturated dinitrogen complexes in solid nitrogen from their M−N stretching frequencies and nitrogen isotopic shifts.[14−16] A major product in the Sc experiments is the rhombic ring $(ScN)_2$, which is formed by reaction of two Sc atoms with one dinitrogen molecule and is relevant to the nitrogen fixation problem.

The important role of transition metal centers in the nitrogen fixation process has been the goal of much significant research. A lot of this work has involved coordination chemistry of Mo, V, and Fe as related to the function of the active center of nitrogenase.[17] End-on and side-on bonding of dinitrogen to early transition-metal dinuclear complexes has been explored, particularly with zirconium.[18,19] Dinitrogen cleavage by Mo(III) complexes has recently been reported.[20] It is clear from these and many other works that two metal centers may be required for efficient cleavage of the dinitrogen molecule. We report here simple reactions of naked scandium atoms with N_2 and show that two Sc atoms can react with N_2 to form the rhombic molecule $(ScN)_2$ where the dinitrogen bond is broken.

Experimental Section

The technique for laser ablation of transition metal atoms and FTIR matrix investigation of reaction products has been described in detail

[†] University of Virginia.
[‡] NASA Ames Research Center.

(1) Douglas, A. E.; Veillette, P. J. *J. Chem. Phys.* **1980**, *72*, 5378.
(2) Fletcher, D. A.; Scurlock, C. T.; Jung, K. Y.; Steimle, T. C. *J. Chem. Phys.* **1993**, *99*, 4288.
(3) Simard, B.; Masoni, C.; Hackett, P. *J. Mol. Spectrosc.* **1989**, *136*, 44.
(4) Peter, S. L.; Dunn, T. M. *J. Chem. Phys.* **1989**, *90*, 5333.
(5) Balfour, W. J.; Qian, C. X. W.; Zhou, C. *J. Chem. Phys.* **1997**, *106*, 4383; *107*, 4473.
(6) Gingrich, R. A. *J. Chem. Phys.* **1968**, *49*, 19.
(7) Ram, R. S.; Bernath, P. F. *J. Chem. Phys.* **1992**, *96*, 6344.
(8) Dismukes, J. P.; Yim, W. M.; Ban, V. S. *J. Cryst. Growth* **1972**, *13/14*, 365
(9) Khaldis, E.; Zeurcher, C. *Helv. Phys. Acta* **1974**, *47*, 421.
(10) Kunze, K. L.; Harrison, J. F. *J. Am. Chem. Soc.* **1990**, *112*, 3812. Harrison, J. F. *J. Phys. Chem.* **1996**, *100*, 3513.
(11) Jeung, G. H.; Koutecky, J. *J. Chem. Phys.* **1988**, *88*, 3747.
(12) Chertihin,. G. V.; Andrews, L.; Rosi, M.; Bauschlicher, C. W., Jr. *J. Phys. Chem. A.* **1997**, *101*, 9085.
(13) Chertihin, G. V.; Andrews, L.; Neurock, M. *J. Phys. Chem.* **1996**, *100*, 14609.
(14) Andrews, L.; Bare, W. D.; Chertihin, G. C. *J. Phys. Chem. A* **1997**, *101*, 8417.
(15) Kushto, G. P.; Souter, P. F.; Chertihin, G. C.; Andrews, L. To be published.
(16) Andrews, L.; Citra, A.; Chertihin, G. V.; Bare, W. D.; Neurock, M. *J. Phys. Chem. A.* To be published.
(17) Richards, R. L. *Coord. Chem. Rev.* **1996**, *154*, 83 and references therein.
(18) Cohen, J. D.; Mylvaganam, M.; Fryzuk, M. D.; Loehr, T. M. *J. Am. Chem. Soc.* **1994**, *116*, 9329.
(19) Fryzuk, M. D.; Haddad, T. S.; Mylvaganam, M.; McConville, D. H.; Rettig, S. *J. Am. Chem. Soc.* **1993**, *115*, 2782.
(20) Laplaza, C. E.; Johnson, M. J. A.; Peters, J. C.; Odom, A. L.; Kim, E.; Cummins, C. C.; George, G. N.; Pickering, I. J. *J. Am. Chem. Soc.* **1996**, *118*, 8623 and references therein.

S0002-7863(97)03701-3 CCC: $15.00
Published on Web 03/18/1998

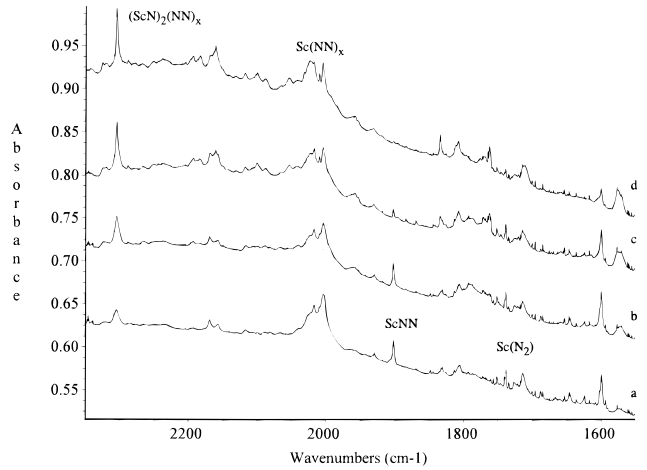

Figure 1. Infrared spectra in the 2350−1550 cm^{-1} region for laser-ablated scandium atoms deposited with 2% N_2 in argon: (a) after deposition for 1 h at 10 K; (b) after annealing to 25 K; (c) after annealing to 30 K; (d) after annealing to 40 K.

previously.[12−14,21−23] The scandium target (Johnson-Matthey, lump) was mounted on a rotating (1 rpm) stainless steel rod. The Nd:YAG laser fundamental (1064 nm, 10 Hz repetition rate, 10 ns pulse width) was focused on the target through a hole in a CsI cryogenic (10 K) window. Laser power ranged from 40 to 50 mJ/pulse at the target. Metal atoms were co-deposited with 1−2% N_2/Ar mixtures or with pure N_2 (and isotopic modifications and mixtures) for 1−2 h periods. FTIR spectra were recorded with 0.5 cm^{-1} resolution and ±0.1 cm^{-1} frequency accuracy on a Nicolet 750 spectrometer using a 77K MCTB detector. Matrix samples were annealed as quickly as possible, and more spectra were collected; selected samples were subject to broadband photolysis by a medium-pressure mercury arc (Philips, 175 W) with globe removed (240−580 nm).

Results

FTIR spectra of the Sc + N_2 reaction products in solid Ar and N_2 and DFT calculations on product molecules will be presented. One feature of these systems is that some bands in argon matrices are almost unshifted from their nitrogen matrix counterparts. Nitrogen isotopic substitution was employed for band identification; isotopic shifts will be discussed in the next section together with band assignments. All systems revealed weak bands for scandium monoxides and dioxides and complexes of monoxides with nitrogen owing to oxide contamination on the scandium target surface.[12] In solid nitrogen, the strong 1657.7 cm^{-1} N_3 radical band was observed.[24,25]

Sc + N_2 Diluted in Ar. Product absorptions for Sc + N_2 in argon are shown in Figures 1−3 and are listed in Table 1. Deposition revealed important absorptions at 2304.9, 2160.4, 2004.1, 1902.0, 1833.8, 1807.3, 1714.0, and 1599.1, in the upper region, which is shown in Figure 1. Significant absorptions appear at 913.0, 898.4, 807.3, 772.2/769.1, and 672.9/668.2 cm^{-1} in the lower region. Figure 2 shows spectra for reaction products in the 930−830 cm^{-1} region using a statistically scrambled $^{14}N_2$:$^{14}N^{15}N$:$^{15}N_2$ sample, and the $^{14}N_2$ reaction product spectrum from 820 to 620 cm^{-1} is illustrated in Figure 3. Annealing decreased the 1902.0 cm^{-1} band, increased all other bands, and produced new 1833.8/1807.3 and 1572.7 cm^{-1} absorptions in the high-frequency region. Annealing first

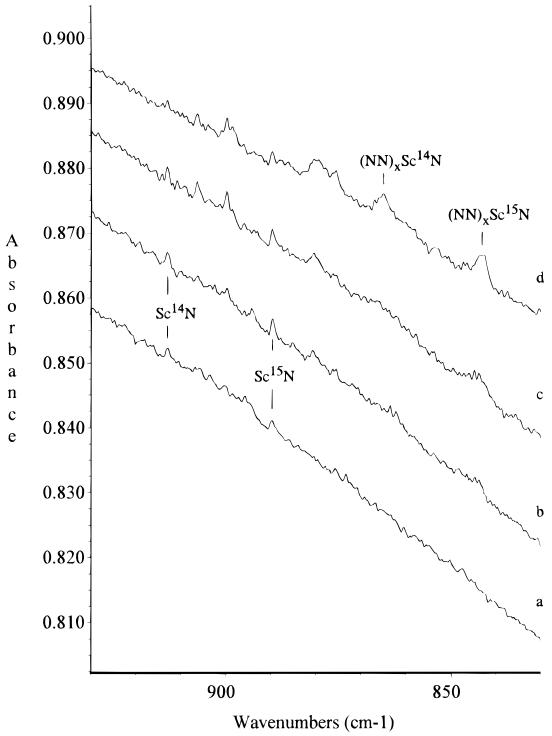

Figure 2. Infrared spectra in the 930−830 cm^{-1} region for laser-ablated scandium atoms deposited with 2% N_2 ($^{14}N_2$/$^{14}N^{15}N$/$^{15}N_2$ = 1/2/1) in argon: (a) after deposition for 1.5 h at 10 K; (b) after annealing to 25 K; (c) after annealing to 30 K; (d) after annealing to 35K.

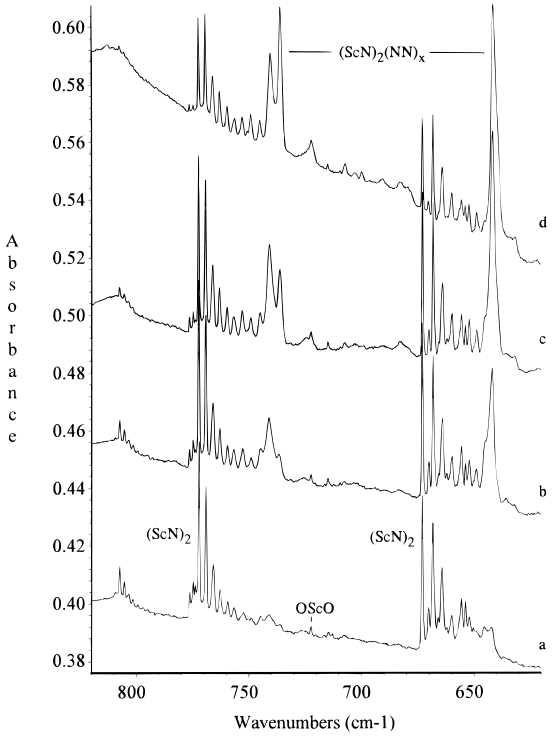

Figure 3. Infrared spectra in the 820−620 cm^{-1} region for laser-ablated scandium atoms deposited with 2% N_2 in argon: (a) after deposition for 1 h at 10 K; (b) after annealing to 25 K; (c) after annealing to 30 K; and (d) after annealing to 40 K.

increased the sharp 913.0 cm^{-1} band, then the 898.4 cm^{-1} band, and finally the broader 865.0 cm^{-1} band. These absorptions gave nitrogen isotopic doublets with the scrambled reagent in Figure 2. The doublets at 772.2/769.1 and 672.9/668.2 cm^{-1} increased on annealing to 25K and decreased on annealing to

(21) Andrews, L.; Chertihin, G. V.; Ricca, A.; Bauschlicher, C. W., Jr. *J. Am. Chem. Soc.* **1996**, *118*, 467.
(22) Thompson, C. A.; Andrews, L. *J. Am. Chem. Soc.* **1996**, *118*, 10242.
(23) Lanzisera, D. V.; Andrews, L. *J. Am. Chem. Soc.* **1997**, *119*, 6392.
(24) Tiam, R.; Facelli, J. C.; Michl, J. *J. Phys. Chem.* **1988**, *92*, 4073
(25) Hassanzadeh, P.; Andrews, L. *J. Phys. Chem.* **1992**, *96*, 9177.

Table 1. Absorptions (cm^{-1}) Observed in Reaction of Scandium Atoms with Nitrogen on Condensation with Excess Argon at 10 K

$^{14}N_2$	$^{15}N_2$	*R* (14/15)	anneal	assignment
2304.9[a]	2227.8	1.0346	++	$(NN)_x(ScN)_2$
2182.9	2110.5	1.0343	+	$(NN)_xSc(N_2)$
2160.4	2089.0	1.0342	+	$(NN)_xSc(N_2)$
2017	1950	1.0343	+	$Sc(NN)_x$
2004.1	1937.8	1.0342	+	$Sc(NN)_x$
1902.0[b]	1839.0	1.0343	−	ScNN
1833.8	1772.7	1.0345	+	$(NN)_xSc(N_2)$
1807	1748	1.0347	+	$(N_x)Sc(N_2)$
1714.0	1657.2	1.0343	+	$Sc(N_2)$?
1599.5	1547.6	1.0335	+	$Sc(N_2)_2Sc$
1572.7	1521.2	1.0340	+	$Sc(N_2)_2Sc$
976.3	976.3			ScO blue site
954.8	954.8			ScO red site
913.0[c]	889.7	1.0262	−	ScN
898.4	875.5	1.0262	+	$(NN)_xScN$
865.0[c]	843.2	1.0261	+	$(NN)_xScN$
807.3[d]	787.0	1.0258	−	$(ScN)_2^+$ isolated (b_{2u})
805.2	785.0	1.0257	−	$(ScN)_2^+$ plus NN
803.3	783.3	1.0255	−	$(ScN)_2^+$ plus NN
772.2[e]	752.6	1.0260	+,−	$(ScN)_2$ isolated (b_{2u})
769.1[e]	749.5	1.0262	+,−	$(ScN)_2$ plus NN
766.0[e]	776.4	1.0263	+,−	$(ScN)_2$ plus NN
763.1	743.4	1.0265	+,−	$(ScN)_2$ plus NN
759.7	740.1	1.0265	+	$(ScN)_2$ plus NN
756.4	737.4	1.0258	−	$(ScN)_2$ plus NN
753.0	733.4	1.0267	−	$(ScN)_2$ plus NN
749.2	729.3	1.0273	+	$(ScN)_2$ plus NN
745.1	725.6	1.0269	+	$(ScN)_2$ plus NN
740.3[e]	721.4	1.0262	++	$(ScN)_2(NN)_x$ saturated (b_{2u})
735.9[e]	717.0	1.0264	++	$(ScN)_2(NN)_x$ site
722.3		1.0257	+	OScO
672.9[e]	656.0	1.0258	+,−	$(ScN)_2$ isolated (b_{3u})
668.2[e]	651.3	1.0259	+,−	$(ScN)_2$ plus NN
664.1[e]	647.2	1.0261	+,−	$(ScN)_2$ plus NN
659.9	643.0	1.02631	+,−	$(ScN)_2$ plus NN
655.6	638.9	1.0261	+	$(ScN)_2$ plus NN
654.0	637.0	1.0264	+	$(ScN)_2$ plus NN
652.2	635.4	1.0264	+	$(ScN)_2$ plus NN
648.9[e]	632.2	1.0264	+	$(ScN)_2$ plus NN
641.3[e]	625.1	1.0259	++	$(ScN)_2(NN)_x$ saturated (b_{3u})
590.5[c]	575.4	1.0262	−	?

[a] Doublet with $^{14}N_2 + {}^{15}N_2$ and triplet 2304.9/2266.6/2227.8 cm^{-1} with $^{14}N_2 + {}^{14}N^{15}N + {}^{15}N_2$. [b] Doublet with $^{14}N_2 + {}^{15}N_2$ and quartet 1902.0/1872.0/1869.4/1839.0 cm^{-1} with $^{14}N_2 + {}^{14}N^{15}N + {}^{15}N_2$. [c] Doublets with both mixtures. [d] Doublets with $^{14}N_2 + {}^{15}N_2$ and triplets 807.3/797.3/787.0 and 805.2/795.1/785.0 cm^{-1} with $^{14}N_2 + {}^{14}N^{15}N + {}^{15}N_2$. [e] Doublets with $^{14}N_2 + {}^{15}N_2$ and triplets with $^{14}N_2 + {}^{14}N^{15}N + {}^{15}N_2$ at 772.2/762.7/752.6, 769.1/759.8/749.5, 766.0/756.3/746.4, 740.3/731.0/721.4, 735.9/726.4/717.0, 672.9/663.0/656.0, 668.2/658.3/651.3, 664.1/654.1/647.2, 641.3/631.3/625.4 cm^{-1}.

higher temperatures while 740.3/735.9 and 641.3 cm^{-1} bands appeared in the spectra (Figure 3). On annealing intensities of the 772.2/769.1 and 672.9/668.2 cm^{-1} absorptions are changed in the same proportion; the new 2304.9, 740.3/735.9, and 641.3 cm^{-1} bands also showed the same correlation. Spectra with mixed $^{14}N_2 + {}^{15}N_2$ samples gave doublets, i.e., the sum of pure isotopic spectra, but reactions with statistically scrambled $^{14}N_2 + {}^{14}N^{15}N + {}^{15}N_2$ gave triplets with new mixed intermediate components as listed in Table 1 (Figure 4). In other experiments annealing to 25 K increased the 772.1/769.1 and 672.9/668.2 cm^{-1} bands by 50% and produced the 740.3 and 641.3 cm^{-1} bands and decreased the 807.3/805.2 cm^{-1} bands by 30%.

Sc + N_2. In solid nitrogen, weak 2300 cm^{-1}, strong 2177.6 cm^{-1}, broad 2003 cm^{-1}, and strong 1699.4 cm^{-1} bands and weak 1759.5, 864.8, 740.3, and 641.2 cm^{-1} absorptions were observed (Table 2). The 2300 cm^{-1} band system and the 739.2 and 641.2 cm^{-1} bands markedly increased on annealing in the same proportion (Figure 5). The 1699.4 cm^{-1} absorption increased then decreased on the annealing sequence. Annealing also produced sharp weaker bands at 921.8 and 832.7 cm^{-1}. The 1759.5 cm^{-1} band and 1762.2 and 1754.4 cm^{-1} satellites increased on annealing and photolysis, while the 864.8 cm^{-1} absorption increased on annealing and decreased on photolysis, which increased a 857.4 cm^{-1} feature. We emphasize here that the 2300, 864.8, 740.3, and 641.2 cm^{-1} bands almost coincide with respective argon matrix counterparts and the 1699.4 cm^{-1} band is just 14.6 cm^{-1} below the 1714.0 cm^{-1} argon matrix band.

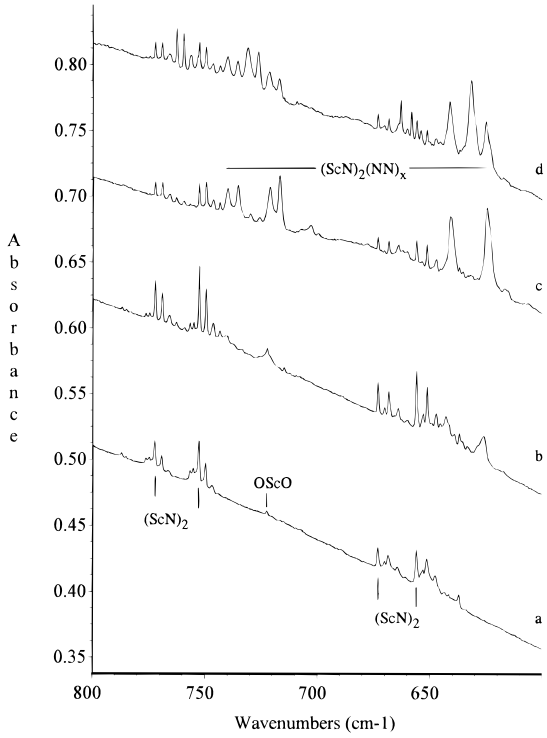

Figure 4. Infrared spectra in the 800−600 cm^{-1} region for laser-ablated scandium atoms with 2% mixed isotopic nitrogen in argon: (a) 1% $^{14}N_2$ + 1% $^{15}N_2$, after deposition for 1 h; (b) sample a, after annealing to 25 K; (c) sample b after annealing to 40 K; (d) 0.5% $^{14}N_2$ + 1% $^{14}N^{15}N$ + 0.5% $^{15}N_2$ after deposition for 1.5 h *and* annealing to 35K.

Figure 6c,d shows the spectrum from a mixture of $^{14}N_2$ and $^{15}N_2$. Most absorptions contained only the two pure isotopic components, but the 2177.6 and 1759.5 cm^{-1} bands revealed new intermediate (i.e. mixed) components and the 739.2 and 641.2 cm^{-1} band systems exhibited weak intermediate isotopic counterparts at 729.9 and 631.6 cm^{-1}. Note that, on annealing, the latter mixed isotopic bands increased relative to the pure isotopic bands. Figure 6a,b shows the analogous spectrum from a statistical $^{14}N_2 + {}^{14}N^{15}N + {}^{15}N_2$ sample. Note that the intermediate components are now stronger than the pure isotopic components, which is more clearly seen after annealing.

DFT Calculations. Density functional theory calculations were performed for small scandium nitride molecules using the BP86 functional in the Gaussian 94 program system employed for scandium oxides.[12,26] The 6-31+G* basis set is used for

(26) Gaussian 94, Revision B.1. Frisch, M. J.; Trucks, G. W.; Schlegel, H. B.; Gill, P. M. W.; Johnson, B. G.; Robb, M. A.; Cheeseman, J. R.; Keith, T.; Petersson, G. A.; Montgomery, J. A.; Raghavachari, K.; Al-Laham, M. A.; Zakrzewski, V. G.; Ortiz, J. V.; Foresman, J. B.; Cioslowski, J.; Stefanov, B. B.; Nanayakkara, A.; Challacombe, M.; Peng, C. Y.; Ayala, P. Y.; Chen, W.; Wong, M. W.; Andres, J. L.; Replogle, E. S.; Gomperts, R.; Martin, R. L.; Fox, D. J.; Binkley, J. S.; Defrees, D. J.; Baker, J.; Stewart, J. P.; Head-Gordon, M.; Gonzalez, C.; Pople J. A. (Gaussian, Inc., Pittsburgh, PA, 1995).

Table 2. Absorptions (cm^{-1}) Observed in Reaction of Scandium Atoms with Nitrogen on Condensation with Excess Nitrogen at 10K

$^{14}N_2$	$^{15}N_2$	$^{14}N_2+^{14}N^{15}N+^{15}N_2$	R (14/15)	anneal	assignment
2327.6	2249.8		1.0346	−	N_2
2306.6	2229.6	2306.6,2267.4,2229.6	1.0345	+	$(ScN)_2(NN)_x$
2300.8	2223.6	2300.8,2262.5,2223.6	1.0347	+	$(NN)_xScN$
2298.6	2221.0	2298.6,2260.7,2222.0	1.0345	+	$(NN)_xScN$
2294.9	2218.4	2295.4,2254.9,2218.3	1.0345	+	$(NN)_XScN$
2291.0	2214.6	2289.5,2253.3,2213.4	1.0345	+	site
2177.6	2105.0	2177, 2156, 2142, 2121, 2106	1.0345	+	$(NN)_x$ $Sc(N_2)$
2114.8	2045.0		1.0341	+, −	?
2112.0	2042.6		1.0340	+, −	?
2026	1959		1.034	+	$Sc(NN)_x$
2004	1938		1.034	+	$Sc(NN)_x$
1966.1	1900.7		1.0344	+, −	$Sc(NN)_x$
1955.2	1890.3		1.0343	+, −	$Sc(NN)_x$
1925.3	1861.4		1.0343	+, −	$Sc(NN)_x$
1907.0	1844.1		1.0341	+, −	$Sc(NN)_x$
1762.2	1703.8	1744.5,1733.4, 1721.1,1715.2	1.0343	+	$(N_2)Sc(N_2)$
1759.5	1701.2	1741.7,1730.6, 1718.5,1712.5	1.0343	+	$(N_2)Sc(N_2)$
1757.4	1699.2	1739.7,1728.6,1716.3,1710.6	1.0343	+	$(N_2)Sc(N_2)$
3373.7	3261.8	3371.8,3318.0,3262.5	1.0340	+,−	$(NN)_xSc(N_2)$
3368.5	3258.2		1.0339	+,−	$(NN)_xSc(N_2)$
1701.2	1644.5		1.0345	+,−	$(NN)_xSc(N_2)$
1699.4	1643.4	1699.0,1671.6,1643.6	1.0341	+,−	$(NN)_xSc(N_2)$
1657.7	1603.3		1.0339	−	N_3
921.8	895.2	921.8,895.2	1.0297	+	$((NN)_xSc_2N)$
868.7	846.4		1.0263	+,−	$(NN)_xScN$
864.8	842.6	864.9,842.7	1.0263	+	$(NN)_xScN$
864.2	842.1	864.2,842.0	1.0262	+	$(NN)_xScN$
863.1	840.9	863.1,840.9	1.0264	+	$(NN)_xScN$
857.4	835.4	857.3,835.4	1.0262	−	$(NN)_xScN$
832.7	813.8	833, 826, 817, 814	1.0232	+	?
812.8	792.5		1.0256	+	? $(x)ScN$
811.8	791.1		1.0262	+	? $(x)ScN$
739.2	720.3	739.2,729.9,720.3	1.0264	+	$(ScN)_2(NN)_x$ (b_{2u})
738.5	719.5	738.2,728.5,717.2	1.0262	+	site
645.6	629.1	645.2,635.2,628.8	1.0262	+	site
641.2	624.8	641.0,631.6,624.8	1.0262	+	$(ScN)_2(NN)_x$ (b_{3u})

nitrogen.[27] For Sc [8s 4p 3d] contraction of the (14s 9p 5d) primitive set developed by Wachters was employed.[28] The s and p spaces are contracted using contraction number 3, while the d space is contracted (311). To this basis set one diffuse p function with exponent 0.13462 is added; this is the tight function optimized by Wachters multiplied by 1.5. The second, more diffuse, p function is not included as it was found to affect results very slightly, but introduced severe convergence problems to the orbital optimization procedure. The Hay diffuse d function with exponent 0.0588 is also added.[29]

First, ScN was calculated to have the $^1\Sigma^+$ ground state with 1.678 Å bond length and 930 cm^{-1} harmonic frequency. For this state MCSCF calculations obtained 748 cm^{-1} and 1.768 Å and later MCSCF/MRCI calculations revealed 774 cm^{-1} and 1.762 Å values.[10] Rotational analysis provided a 1.687 Å bond length.[7] We will show below that the ScN frequency in solid argon is 913 cm^{-1}, which we suspect is within 10 cm^{-1} of the gas phase value. Clearly DFT/BP86 calculations give a better representation of the ScN molecule bond length and vibrational frequency. Considerable success in predicting vibrational frequencies has been found recently for DFT/BP86 calculations with beryllium[23] and transition metal systems.[12,30−32]

The singlet complex (NN)ScN is bound by 13.3 kcal/mol and the Sc−N stretching fundamental is 911 cm^{-1}. The next complex in the series, $(NN)_2ScN$, is bound by 25.3 kcal/mol and the Sc−N fundamental is 882 cm^{-1}. Note (Table 3) that the infrared intensity of the Sc−N fundamental increases with ligation by dinitrogen at scandium.

The rhombic dimer $(ScN)_2$ has a ^1A_g ground state and is bound by 142 kcal/mol with respect to two ScN molecules. Calculated frequencies are given in Table 3. The $^3B_{2u}$ state of $(ScN)_2$ and the $^2B_{2u}$ state of $(ScN)_2^+$ are 29.2 and 144.3 kcal/mol higher, respectively.

Three ScN_2 species were calculated: the linear ScNN quartet is the global minimum with the side-bound quartet 2.5 kcal/mol higher, and the linear doublet NScN is 92 kcal/mol higher. The diagnostic N−N stretching modes were calculated at 1870 and 1744 cm^{-1}, respectively, for ScNN and $Sc(N_2)$. Three $Sc(N_2)_2$ species were considered: the linear quartet is the most stable, more stable than N_2 + ScNN by 20.1 kcal/mol.

The Sc $3d^14s^2$ occupation is lower than the $3d^24s^1$ occupation, but the doubly occupied 4s orbital results in a much larger Sc−NN repulsion for the $3d^14s^2$ occupation than for the $3d^24s^1$ occupation. This leads to a longer Sc−NN distance for the $3d^14s^2$ occupation. The d to π^* donation is natually smaller for the $3d^14s^2$ occupation because of the longer Sc−N distance and because there is only one d electron available to donate to N_2. Thus promotion to $3d^24s^1$ is favored for ScNN and $Sc(N_2)$. The bonding in the $^4\Sigma^-$ state of ScNN arises from the $3d^24s^1$ occupation of Sc. The dπ orbital donates charge to the N_2 π^* orbital and the N_2 donates charge to the Sc in the σ space. The 4s orbital mixes with both the Sc 4p and 3d σ orbitals to

(27) Frisch, M. J.; Pople, J. A.; Binkley, J. S. *J. Chem. Phys.* **1984**, *80*, 3265 and references therein.
(28) Wachters, A. J. H. *J. Chem. Phys.* **1970**, *52*, 1033.
(29) Hay, P. J. *J. Chem. Phys.* **1977**, *66*, 4377.
(30) Fournier, R. *J. Chem. Phys.* **1993**, *99*, 1801.
(31) Jones, V.; Thiel, W. *J. Chem. Phys.* **1995**, *102*, 8474.
(32) Rosi, M.; Bauschlicher, C. W., Jr.; Chertihin, G. V.; Andrews, L. *Theor. Chem. Acc.* **1998**. In press.

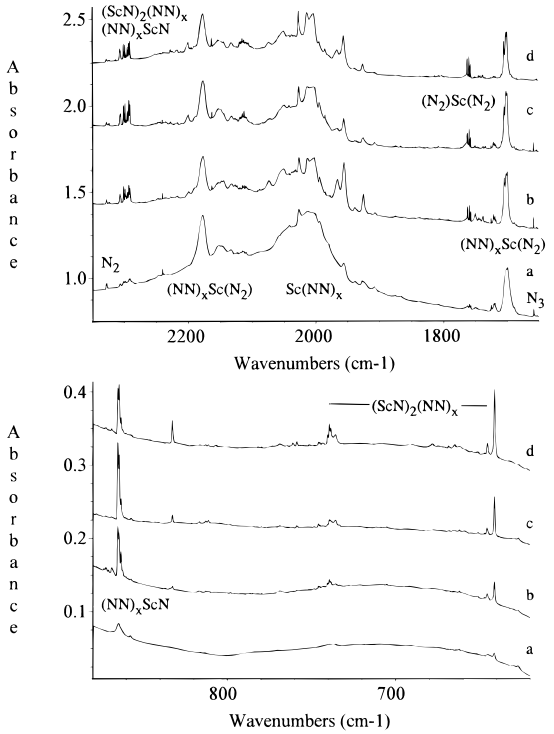

Figure 5. Infrared spectra in the 2350−1650 and 880−620 cm^{-1} regions for laser-ablated Sc atoms deposited with pure nitrogen: (a) deposition for 2 h at 10 K; (b) after annealing to 25 K; (c) sample b after annealing to 30 K; (d) sample c after annealing to 40 K.

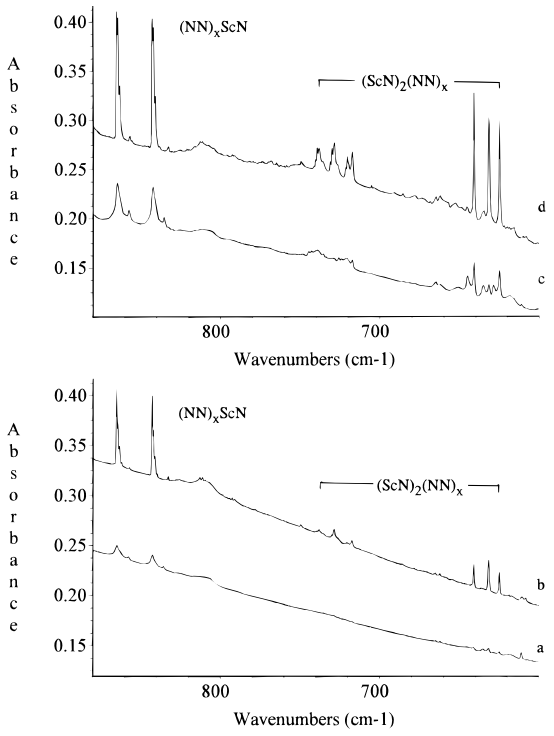

Figure 6. Infrared spectra in the 880−600 cm^{-1} region for lasser-ablated Sc atoms deposited with mixed isotopic nitrogen: (a) $^{14}N_2/^{14}N^{15}N/^{15}N_2$ = 1/2/1 sample deposited for 1 h; (b) sample a after annealing to 35 K; (c) $^{14}N_2/^{15}N_2$ = 1/1 sample deposited for 1.5 h; (d) sample c after annealing to 35 K.

polarize away from the N_2 and hence reduce the Sc−NN repulsion.

Bonding in the $^4\Sigma_g^-$ state of NNScNN is very similar to that in the $^4\Sigma^-$ state of ScNN. With N_2 molecules on both sides of the Sc, only sd σ hybridization occurs for NNScNN. Thus the 4s population is smaller for NNScNN than ScNN (0.98 vs 1.18 electrons). The bonding mechanism is very similar for the $^4B_1$ state of $Sc(N_2)$. The N_2 π^* orbitals are of b_2 and a_2 symmetry, and therefore these are the two symmetries that contain the open-shell d orbitals. The third open-shell is natually the Sc 4s(a_1) orbital.

Table 3. Harmonic Frequencies and Bond Distances Calculated for Scandium Nitrides Using DFT/BP86

molecule	distances, Å	frequencies, cm^{-1} (intensities, km/mol)
ScN, $^1\Sigma$	1.678	930 (10)
(NN)ScN	1.130, 2.259, 1.703	911 (48), 2188 (503)
$(NN)_2ScN$	1.128, 2.279, 1.723	882 (71), 2190 (848), 2213 (210)
ScNN, $^4\Sigma^-$	2.015, 1.167	1870 (688), 412 (14), 260 (2)
$E = 0.0^a$		
$Sc(N_2)$, $^4B_1$	2.147, 1.195	1744 (376), 363 (2), 350 (18)
$E = +2.5$		
NScN, $^2\Pi_u$	1.763	662 (0), 359 (63), 132 (213)
$E = +92$		
$(ScN)_2$, ^1A_g	1.895	792 (176), 735 (0), 651 (223),
$E = 0.0^a$		474 (0), 431 (0), 254 (112)
$(ScN)_2$, $^3B_{2u}$	1.915	701 (0), 672 (1797), 527 (52),
$E = +29.2$		525 (0), 363 (0), 54 (30)
$(ScN)_2^+$, $^2B_{2u}$	1.900	838 (220), 730 (0), 542 (64),
$E = +144.3$		521 (0), 385 (0), 204 (151)
$Sc(NN)_2$, $^4\Sigma_g^-$ linear	2.114, 1.151	2043 (0), 1961 (2720),
$E = 0.0^a$		375 (2), 367 (91)
(NN)Sc(N_2), $^4A''$, planar		2026 (687), 1859 (786),
$E = +5.6$		390 (0.1), 353 (1)
$Sc(N_2)_2$, $^4B_1$, D_{2d}	2.199, 1.193	1794 (0), 1756 (1239),
$E = +5.8$		377 (13), 328 (40)

[a] Relative energies of structural isomers in kcal/mol.

The bonding in the $^2\Pi_u$ state of NScN is very different from that in $Sc(N_2)$ and ScNN. The valence occupation, ie that without the N 1s and 2s orbitals and the Sc 1s−3p orbitals, is $(\sigma_g)^2(\pi_g)^4(\pi_u)^3$. That is, N 2p$\sigma$ and Sc 3dσ orbitals form a three-center−two-electron bond. The N 2pπ and Sc 3dπ orbitals form similar three-center bonds. The π_u orbitals are essentially localized on the N atoms. This bonding mechanism implies that Sc is $3d^3$, which is very high in energy. However the Sc donates almost an entire electron to the two N atoms. The doublet state arsing from 4s4p hybridization of Sc, yielding a $(\sigma_g)^2$ $(\sigma_u)^2(\pi_g)^4(\pi_u)^1$ occupation, is higher in energy, because the optimal bond distance for the Sc 4s and 3d orbitals is different. Thus this occupation yields two good σ bonds, but the π bonding is weak and hence is above the $^2\Pi_u$ state with the $(\sigma_g)^2(\pi_g)^4(\pi_u)^3$ occupation. We should note that we have found linear quartet states below the $^2\Pi_u$ state, but these have imaginary frequencies.

Discussion

Infrared spectra of scandium nitrides will be assigned with the help of isotopic substitution and DFT calculations.

ScN. The sharp weak band at 913.0 cm^{-1} in solid argon containing 2% N_2 increased then decreased on annealing cycles, giving way first to a band at 898.4 cm^{-1} and then finally to a broader band at 865.0 cm^{-1} (Figure 2). These bands exhibited one nitrogen-15 component and 14/15 isotopic ratios 1.0262 ± 0.0001, which is just under the harmonic diatomic value (1.0264) and appropriate for the Sc−N fundamental vibration with small cubic anharmonicity. In solid nitrogen an 864.8 cm^{-1} band increased in absorbance and structure on annealing in parallel with a set of bands near 2300 cm^{-1} (Figure 4). The former

band showed a single nitrogen-15 counterpart at 842.6 cm^{-1} with the 14/15 ratio of 1.0263 and the latter band gave triplets with scrambled $^{14,15}N_2$ (Table 2) with the 14/15 ratio of 1.0346 ± 0.0001. The former band is clearly due to an Sc−N vibration and the latter band is due to a dinitrogen vibration. These bands are appropriate for a $(NN)_xScN$ complex where *x* could, in principle, be as large as six. The 898.4 cm^{-1} band in solid argon containing 2% N_2 is due to an incompletely saturated $(NN)_xScN$ complex ($x < 6$). Note agreement between the much weaker 865.0 cm^{-1} band formed on annealing in solid argon and the stronger 864.8 cm^{-1} band in solid nitrogen for the $(NN)_x$-ScN species. Photolysis decreased the 864.8 cm^{-1} band in favor of a sharp new 857.4 cm^{-1} feature, but further annealing increased the 864.8 cm^{-1} band and decreased the 857.4 cm^{-1} band.

The 913.0 cm^{-1} band in solid argon is assigned to isolated ScN. This band is in excellent agreement with the 930 cm^{-1} DFT/BP86 calculation but substantially higher than the 774 cm^{-1} MCSCF/MRCI value[10] and the 795 cm^{-1} frequency predicted from empirical correlation with bond length.[7] Furthermore, the excellent agreement between the DFT/BP86 bond length and the gas-phase value[7] bodes well for the BP86 prediction of fundamental frequency. On the basis of agreement between the gas phase (1039.6 cm^{-1}) and argon matrix (1032.4 cm^{-1}) fundamentals[1,15] for TiN and the gas phase (1020 ± 5 cm^{-1}) and argon matrix (1026.2 cm^{-1}) fundamentals[3,14] for VN, the gas-phase fundamental for ScN is predicted to be in the 920−910 cm^{-1} range.

A similar situation exists for the CrN molecule where DFT/BPL predicts a 1017 cm^{-1} fundamental for the $^4\Sigma^-$ ground state, substantially higher than the 854 cm^{-1} MCSCF value but in excellent agreement with the recent 1044 cm^{-1} argon matrix and approximate 1000 ± 100 cm^{-1} gas-phase fundamentals.[5,10,14] Likewise the DFT/BPL predicted 1.555 Å bond length for CrN is in much better agreement with the recent 1.563 Å measurement from rotational analysis than the 1.619 Å MCSCF value.[5,10,14] In contrast the DFT and MCSCF calculations both predict frequencies for TiN and VN in very good agreement with gas phase and matrix determinations.[1−3,10,14,15]

Similar behavior has been observed for TiN, VN, CrN and their dinitrogen complexes.[14,15] In the case of VN, five distinct $(NN)_xVN$ complexes were observed culminating in the most extensively ligated species absorbing at 997.0 cm^{-1} in solid nitrogen and 997.8 cm^{-1} after annealing in solid argon.

DFT calculations done to model the dinitrogen complexes for (NN)ScN and $(NN)_2ScN$ show that the Sc−N fundamental red-shifts and gains intensity with ligation in agreement with experiment. The N−N fundamentals predicted near 2190 cm^{-1} are observed near 2300 cm^{-1} perhaps because the complexes are more extensively ligated than the model compounds.

We note that the present 913.0 cm^{-1} assignment for ScN in solid argon is near the ScO argon matrix (955 cm^{-1})[12] and gas phase (965 cm^{-1}) values just as the TiN fundamental is near the TiO fundamental (argon matrix, 988 cm^{-1} and gas phase, 1000 cm^{-1}).[33,34]

$(ScN)_2$. The argon matrix spectra are characterized by strong, sharp band series starting at 772.2 and 672.9 cm^{-1} that first increase and then decrease on annealing cycles in favor of strong bands at 740.3 and 641.3 cm^{-1}, which are accompanied by a strong 2304.9 cm^{-1} band. The former bands exhibit ScN diatomic isotopic ratios whereas the latter band shows the ratio for dinitrogen. In the nitrogen matrix, weak analogous 2306.6, 739.2, and 641.2 cm^{-1} bands increase together on annealing (Figure 4) and exhibit 14/15 ratios similar to the argon matrix counterparts.

The two lower bands in both solid argon containing 2% N_2 and pure nitrogen give triplet absorptions with statistical $^{14,15}N_2$ clearly identifying vibrations of two equivalent N atoms. The sharp 772.2 and 672.9 cm^{-1} bands are assigned to the b_{2u} and b_{3u} stretching modes of the isolated rhombic molecule $(ScN)_2$, which requires the ScN diatomic 14/15 isotopic ratio. These assignments are substantiated by the DFT calculations, which predict strong b_{2u} and b_{3u} modes at 792 and 651 cm^{-1} for the ^1A_g ground state, in excellent agreement with the observed values.

The strong 2304.9, 740.3, and 641.3 cm^{-1} bands that appear on annealing in solid argon are due to the N_2-ligated $(ScN)_2$ species denoted $(ScN)_2(NN)_x$ with dinitrogen ligands bonded to both metal centers. Although the 2304.9 cm^{-1} band gives a triplet absorption with $^{14,15}N_2$, the dinitrogen ligands could be end-bonded. The series of eight resolved bands leading from 772.2 to 740.3 cm^{-1} and seven resolved bands from 672.9 to 641.3 cm^{-1} are best explained by successively increasing numbers of dinitrogen ligands at each Sc position in the $(ScN)_2$ ring. We must note that if each Sc atom can attain 6-fold coordination, a total of eight dinitrogen molecules will be required for saturation of $(ScN)_2$ to $(ScN)_2(NN)_x$. The nitrogen matrix spectrum is clearly dominated by the saturated ligated species with nearly the same band positions as the annealed argon matrix.

The rhombic $(MN)_2$ species is also important in the titanium system,[15] but not for the V, Cr, Mn, and Fe reactions with nitrogen.[13,14] The $(MN)_2$ rhombic dimer also appears with Co and Ni.[16] This derives from several factors including the overall yield of MN produced, the yield of MNN intermediate, and the stability of the ligated $(NN)_xMN$ complexes.

The weaker structured 807.3/805.2/803.3 cm^{-1} band system (Figure 3) shows isotopic character just like the stronger 772.2 cm^{-1} band system, but the bands decrease about 30% on 25 K annealing and another 30% on broad-band photolysis, whereas the 772.2 cm^{-1} band increases slightly on 25 K annealing. Similar DFT calculations predict the strongest (b_{2u}) fundamental of the $(ScN)_2^+$ species to appear 46 cm^{-1} higher than this mode for $(ScN)_2$, and the weak 807.3 cm^{-1} band is 35 cm^{-1} above the strong 772.2 cm^{-1} band. Accordingly, the weaker 807.3 cm^{-1} band is probably due to $(ScN)_2^+$. The much weaker b_{3u} mode is predicted in the low 500 cm^{-1} region and is not observed here. The 590.5 cm^{-1} band shows opposite photolysis behavior and cannot be identified.

Work in progress with Sc and Ar/H_2 samples containing a trace of N_2 impurity (<0.1%) deposited at 7 K gives a low yield of the 807.3, 772.2, and 672.9 cm^{-1} bands with only weak 769.1 and 668.2 cm^{-1} satellites. Annealing to 23 K doubles the 772.2 and 672.9 cm^{-1} bands, triples the 769.1 and 668.2 cm^{-1} satellites, and leaves the 807.3 cm^{-1} band unchanged. Final annealing to 38 K decreases the 807.3 cm^{-1} band (to 40%) and the 772.2 and 672.9 cm^{-1} bands (to 70%), slightly increases only the first three (labeled plus NN) satellites, and does not produce the 740.3 and 641.3 cm^{-1} bands. These recent observations provide further support for the above conclusions.

ScN_2. DFT calculations predict that quartet linear ScNN is only slightly more stable than cyclic $Sc(N_2)$; these molecules have strong absorptions calculated at 1870 and 1744 cm^{-1}, respectively. Examination of the argon and nitrogen matrix spectra in this region reveals sharp bands at 1902.0 and 1714.0 cm^{-1} in solid argon and a strong band at 1699.3 cm^{-1} with an associated band at 2177.6 cm^{-1} in solid nitrogen. The sharp 1902.0 cm^{-1} argon matrix band becomes a 1902.0/1872.0/

1869.4/1839.0 cm^{-1} quartet with statistical $^{14,15}N_2$, which indicates two inequivalent nitrogen atoms, but the 1714.0 cm^{-1} band was too weak to observe mixed components. However, the strong 1699.3 cm^{-1} nitrogen matrix band gave a 1699.0/1671.6/1643.6 cm^{-1} triplet, for two equivalent nitrogen atoms, and the associated 2177.6 cm^{-1} band gave a broad pentet with strong median peak using statistical $^{14,15}N_2$. Clearly, the former band involves two equivalent nitrogen atoms, i.e., sideways bonded N_2 and the latter band involves a number of end-bound NN subunits.

Accordingly the 1902.0 cm^{-1} band is assigned to ScNN in solid argon. The 2177.6 and 1699.4 cm^{-1} bands are assigned, respectively, to end-bound NN ligands and the side-bound N_2 complex of $(NN)_xSc(N_2)$ in solid nitrogen. The weak 1714.0 cm^{-1} band is probably the argon matrix counterpart, $Sc(N_2)$, but we cannot be certain. The bands at 1833.8 and 1807 cm^{-1} that grow on annealing appear to be due to partially coordinated $(NN)_xSc(N_2)$ species. The major strong band at 2004 cm^{-1} in both matrixes is probably due to the coordinatively saturated $Sc(NN)_x$ species with x likely to be 6.

The 1699.4 cm^{-1} band reveals splittings on annealing at 1701.2 and 1704.3 cm^{-1} (Figure 5), which are presumably due to different orientations of the $(NN)_x$ ligands or the entire $(NN)_xSc(N_2)$ molecule within the matrix cage; these splittings are matched in behavior by a much weaker band at 3368.5 cm^{-1} (1.3% of the absorbance at 1699.4 cm^{-1}) with splittings at 3372.7 and 3378.5 cm^{-1}. The latter bands are clearly due to overtones of the former bands. This is confirmed by the constant difference (29.9 ± 0.2 cm^{-1}) between the overtone and two times the fundamental and the matching isotopic ratios and statistical mixed isotopic triplet patterns. It is interesting to note that the $^{14}N_2$ components for the fundamental and overtone are slightly different in the statistical isotopic mixture because the dinitrogen ligands are isotopically substituted as well. Such overtone bands have been observed for other $(NN)_xM(N_2)$ species where the product yield was relatively high including Y, Sm, Eu, and Yb; the overtone band may serve as an additional diagnostic for the sideways bound $M(N_2)$ species.[35,36]

Other Absorptions. Two other absorptions show evidence for two dinitrogen subunits. The matrix-split band at 1762.2, 1759.5, and 1757.4 cm^{-1} in solid nitrogen exhibits an intermediate feature at 1721.1, 1718.5, and 1716.3 cm^{-1} with $^{14}N_2 + {}^{15}N_2$ and three new intermediate matrix-split (Table 2) bands using $^{14}N_2 + {}^{14}N^{15}N + {}^{15}N_2$ with 1:4:6:2:4:x intensities relative to the above $^{14}N_2$ trio (the $^{15}N_2$ trio was masked by the strong 1699.3 cm^{-1} $(NN)_xSc(^{14}N_2)$ band). DFT calculations predict the linear NNScNN and D_{2d} $Sc(N_2)_2$ species to have very strong antisymmetric N−N stretching modes at 1961 and 1756 cm^{-1}, respectively. Clearly, agreement with the latter is excellent and the above matrix-split bands are assigned to $Sc(N_2)_2$. The observed spectrum is textbook for a species with two equivalent N_2 subunits and equivalent atomic positions except that the third site-split component is slightly more intense than expected. The major yield of $Sc(N_2)$ in solid nitrogen makes the $Sc(N_2)_2$ species a likely minor product.

The sharp 1599.5 cm^{-1} band in solid argon containing 2% N_2 has a broader 1572.7 cm^{-1} counterpart, which grows on annealing, exhibits a 1548 cm^{-1} intermediate band in $^{14}N_2 + {}^{15}N_2$ experiments, and indicates two dinitrogen molecules. This region is appropriate for (>N═N) bridged dinitrogen, and these bands are tentatively assigned to the $Sc(\mu\text{-}N_2)_2Sc$ ring species.

Finally, sharp weaker bands appear on annealing at 921.8 and 832.7 cm^{-1} in solid nitrogen. The 921.8 cm^{-1} band becomes a sharp unshifted doublet with mixed isotopic precursors and exhibits a higher 14/15 isotopic ratio (1.0297) than the ScN diatomic value. This suggests that a single N is vibrating against a heavier mass than one Sc atom. Accordingly, the weak 921.8 cm^{-1} band is tentatively assigned to Sc_2N, which must be complexed with dinitrogen as $(NN)_xSc_2N$. The 832.7 cm^{-1} band exhibits a 14/15 isotopic ratio (1.0232) and intermediate isotopic components for an aggregate species that cannot be identified without more information.

Reaction Mechanisms. The important step in these reactions of laser-ablated Sc atoms is dissociation of molecular nitrogen to atoms, and this is caused by the impact with energetic Sc atoms from laser ablation.[13,14,37] Similar ablation methods have produced Sc atoms with kinetic energies up to 30 eV.[38] ScN is formed in these experiments by direct atom combination, reaction 1. A similar mechanism was proposed for the

$$Sc + N \rightarrow ScN \qquad (1)$$

production of FeN.[13] The observation of N_3 radical attests to the formation of N atoms in these experiments.[24,25]

Clearly more N atoms are produced in the nitrogen matrix experiments, hence the higher yield of ScN as ligated $(NN)_xScN$ and the observation of N_3 radical in solid nitrogen.

$$xN_2 + Sc + N \rightarrow (NN)_xScN \qquad (2)$$

The mechanism of formation of $(ScN)_2$ is of interest as two transition metal atoms effectively convert N_2 to a nitride, which may assist in understanding the important nitrogen fixation process. In the argon matrix experiments with $^{14}N_2 + {}^{15}N_2$, doublets are observed for the $(ScN)_2$ bands, indicating that a single N_2 molecule is involved in the reaction, which must proceed through an intermediate ScN_2 species, either ScNN or $Sc(N_2)$, as indicated in eq 3. Dimerization of ScN is not the

$$Sc + N_2 + Sc \rightarrow ScN_2 + Sc \rightarrow (ScN)_2 \qquad (3)$$

route in solid argon, as the ScN yield is relatively low in argon matrix experiments. Furthermore, the dimerization mechanism would require a mixed isotopic ($Sc^{14}NSc^{15}N$) component, and such is not observed. Even on annealing, there is a 50% growth of $(Sc^{14}N)_2$ and $(Sc^{15}N)_2$ absorptions but no growth of a mixed isotopic component (Figure 4), and reaction 3 produces more $(ScN)_2$ species on annealing in solid argon.

On deposition with pure $^{14}N_2 + {}^{15}N_2$ (Figure 5c), the major products involve one dinitrogen reagent molecule according to reaction 4. However, on annealing, notice the growth of pure

$$(NN)_xSc(N_2) + Sc \rightarrow (ScN)_2(NN)_x \qquad (4)$$

isotopic products $(Sc^{14}N_2)(NN)_x$ and $(Sc^{15}N_2)(NN)_x$ *and* the mixed isotopic product (Figure 5d), indicating that reaction 4 *and* dimerization reaction 5 both contribute to the product yield in solid nitrogen where the initial yield of $(NN)_xScN$ is high.[39]

$$2\,(NN)_xScN \rightarrow (ScN)_2(NN)_x \qquad (5)$$

(33) Chertihin, G. V.; Andrews, L. *J. Phys. Chem.* **1995**, *99*, 6356.
(34) Merer, A. J. *Annu. Rev. Phys. Chem.* **1989**, *40*, 407.
(35) Chertihin, G. V.; Bare, W. D.; Andrews, L. *J. Phys. Chem. A* In press. Annealing to 35 K destroys the N_3^- trapped in solid nitrogen in laser-ablated Y and La atom experiments.
(36) Willson, S. P.; Andrews, L. To be published.
(37) Kang, H.; Beauchamp, J. L. *J. Phys. Chem.* **1985**, *89*, 3364.
(38) Thiem, T. L.; Salter, R. H.; Gardner, J. A. *Chem. Phys. Lett.* **1994**, *218*, 309.
(39) The product of (4) and (5) contains dinitrogen ligands on *both* Sc centers and could be written as $(NN)_x(ScN)_2(NN)_x$.

The reaction of another Sc atom with $(NN)_xScN$ produces the discandium mononitride species, reaction 6, which following the example of ScN, must be ligated by dinitrogen in the nitrogen matrix.

$$(NN)_xScN + Sc \rightarrow (NN)_xScNSc(NN)_x \qquad (6)$$

Are any of these N_2 reactions possible with thermal Sc atoms? Preliminary thermal Sc atom matrix experiments of Klotzbucher[40] with 10% N_2 in argon reveal weak 2304, 744, and 641 cm^{-1} bands (A = absorbance = 0.02) that are in agreement with the absorptions assigned here to $(ScN)_2(NN)_x$ and the 1833 cm^{-1} band assigned here to $(NN)_xSc(N_2)$ in solid argon. With pure nitrogen, thermal experiments gave the 1699 cm^{-1} band for $(NN)_xSc(N_2)$ in solid nitrogen. However, no bands were observed for ScN or $(NN)_xScN$ species with thermal Sc atoms confirming the need for dissociation of N_2 to form ScN, which is provided by excess energy in the laser-ablated scandium atoms. Thus, the $(ScN)_2$ molecule can be made by reaction 3 or 4 using thermal Sc atoms.

What is the role of electrons or Sc^+ ions from the laser-ablated metal vapor plume in these experiments? The detection of N_3^- at 2003.3 cm^{-1} in similar Y and La experiments[35] in solid nitrogen shows that some charged species survive to reach the matrix.[41] Even if impact with Sc^+ contributes to the dissociation of N_2, most of the metal cation species produced here are probably neutralized during the condensation process. Annealing would almost certainly annihilate any charged species trapped, and the clear growth of $(NN)_xScN$, $(NN)_xSc(N_2)$, $(ScN)_2(NN)_x$, and $(ScN)_2$ on annealing argues strongly that these are neutral species. Any scandium−nitrogen cationic species are expected to be minor contributors to the observed spectrum.

The weak 807.3 cm^{-1} band system that is almost destroyed on annealing is probably due to $(ScN)_2^+$, which can be made by reaction of Sc^+ or by photoionization of $(ScN)_2$ with radiation from the laser plume.

Conclusions

Laser-ablated Sc atoms react with nitrogen to form ScN, $Sc(N_2)$, and $(ScN)_2$ and their N_2 ligated counterparts. These identifications are based on isotopic shifts and agreement with DFT frequency calculations. It is noteworthy that annealed argon matrix samples containing 2% N_2 give almost the same absorptions as nitrogen matrix samples for the ligated complexes $(NN)_xScN$ and $(ScN)_2(NN)_x$. The rhombic $(ScN)_2$ species is made by reaction of a second Sc atom with an intermediate ScN_2 species and, thus, provides an interesting route to nitrogen fixation with naked metal atoms.

Acknowledgment. We gratefully acknowledge the assistance of W. D. Bare with the laser-ablation experiments and the communication of unpublished thermal scandium experimental results by W. Klotzbucher.

JA973701D

(40) Klotzbucher, W. E. Unpublished results.

(41) The very strong $Sc(NN)_x$ band at 2004 cm^{-1} completely masks any N_3^- absorption present here.